Effect of Ag+ on the Excited-State Properties of a Gas-Phase (Cytosine)2Ag+ Complex: Electronic Transition and Estimated Lifetime

Matias Berdakin,[†] Géraldine Féraud,[‡] Claude Dedonder-Lardeux,[‡] Christophe Jouvet,[‡] and Gustavo A. Pino*,[†]

[†]INFIQC (CONICET − UNC), Departamento de Fisicoquímica, Facultad de Ciencias Químicas, Centro Láser de Ciencias Moleculares, Universidad Nacional de Córdoba, Ciudad Universitaria, X5000HUA Córdoba, Argentina

[‡]Physique des Interactions Ioniques et Moléculaires (PIIM), CNRS, Aix Marseille Université: UMR-7345, 13397 Marseille, France

Ⓢ Supporting Information

ABSTRACT: Recently, DNA molecules have received great attention because of their potential applications in material science. One interesting example is the production of highly fluorescent and tunable DNA−Ag_n clusters with cytosine (C)-rich DNA strands. Here, we report the UV photofragmentation spectra of gas-phase cytosine···Ag+···cytosine (C_2Ag^+) and cytosine···H+···cytosine (C_2H^+) complexes together with theoretical calculations. In both cases, the excitation energy does not differ significantly from that of isolated cytosine or protonated cytosine, indicating that the excitation takes place on the DNA base. However, the excited-state lifetime of the C_2H^+ (τ = 85 fs), estimated from the bandwidth of the spectrum, is at least 2 orders of magnitude shorter than that of the C_2Ag^+ (τ > 5000 fs). The increased excited-state lifetime upon silver complexation is quite unexpected, and it clearly opens the question about what factors are controlling the nonradiative decay in pyrimidine DNA bases. This is an important result for the expanding field of metal-mediated base pairing and may also be important to the photophysical properties of DNA-templated fluorescent silver clusters.

SECTION: Spectroscopy, Photochemistry, and Excited States
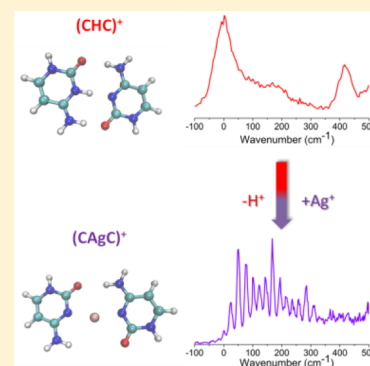
In the past years, natural and artificial DNA molecules have been of great interest because of their potential applications in biological and material science.[1−5] The central idea is to exchange the natural canonical interaction between the DNA bases for new noncovalent interactions (i.e., hydrogen bonding, hydrophobic interactions, structure complementarity, and site-specific functionalization),[6] leading to artificial base pairing. One of the recently established methods for site-specific functionalization is metal-mediated base pairing that is to replace the hydrogen atom within hydrogen-bonded base pairs by metal ions.[6]

Metal-mediated base pairing constitutes a major advance in the attempt of expanding the genetic code; at least 23 artificial metal-mediated base pairs have been reported to stabilize the double helix structure of DNA (for a complete review, the readers are referred to a recent work on metal-mediated DNA base pairs that address all of the studies on this topics over time).[6] Besides, the incorporation of metal-mediated base pairing has proven to be a suitable and powerful tool for the potential development of artificial DNA-based devices.[7,8]

It is recognized that the T−T and C−C (T = thymine; C = cytosine) mismatch pairs can be transformed into very stable T−Hg^{2+}−T[9] and C−Ag^+−C[10,11] metallo-mediated base pairs by incorporating Hg^{2+} or Ag^+ cations, respectively. The strong metal−base interactions are highly specific in both cases, and it

can interfere in the replication and transcription of DNA and induce conformational changes (i.e., from random coil conformation to duplex conformation). These highly specific conformational changes have been used as an analytical probe of Ag^+ upon biorecognition by C−C mismatching by using circular dichroism spectroscopy to sense real time conformational changes[12] or electrochemical methods to follow the conformational-dependent activity of exonuclease III.[13]

One interesting application of the strong nucleobase−metal binding feature of DNA is the production of highly fluorescent and tunable hybrid DNA−Ag_n clusters. The optical properties of these hybrid systems (e.g., high fluorescence yield and absorption/emission wavelength tuning) are strongly dependent on the nucleobases sequence,[14−17] cluster size,[18] pH,[19] temperature,[20] and so forth. These photophysical properties of silver clusters have led to the creation of a new generation of small and biocompatible fluorophores as biological labels, which exceed the commonly used semiconductor quantum dots and organic dyes in regard to fluorescence quantum yield, photostability, and biocompatibility due to the low toxicity and very small size of the Ag_n clusters.[14,21] For more information

about these fascinating systems, the readers are recommended to refer to recent reviews on this topic.[14,22−27]

The hybrid DNA−Ag$_n$ clusters have two intense absorption bands, one in the visible that is tunable with the DNA base sequence and the other in the UV spectral region that is common to all of them, regardless of the position of the visible band.[14,17,19,28] The UV excitation band is located in the spectral region where the DNA bases absorb (260−270 nm). Very interestingly, the excitation of the common UV band leads to the same fluorescence spectrum as that in the case of excitation of the tunable visible band. It was previously suggested that this peak could be due to excitation to higher-lying states;[28] however, recent evidence indicates that the UV absorption band corresponds to excitation of the nucleobases.[17]

While DNA nucleobases[29] and protonated nucleobases[30] present mostly very short excited-state lifetimes on the subpicosecond to picosecond time scale, highly fluorescent DNA−Ag$_n$ clusters have excited-state lifetimes in the nanosecond regime,[10] although according to a previous report,[17] their excitation in the UV spectral region is on the DNA moiety for which short excited-state lifetimes are expected. This is clear evidence of the effect of Ag on the excited-state lifetime of these systems. In addition, it has been reported that the formation of highly fluorescent DNA−Ag$_n$ clusters is favored when using C-rich DNA strands as the template.[15,19]

The detailed mechanism responsible for the fluorescence enhancement is still elusive, and whether metal-mediated DNA base pairs will behave in a similar way as natural DNA may be a major issue to take into account when analyzing biocompatibility. In this context, gas-phase characterization of optical and structural properties of model systems, together with quantum modeling, has shown to be suitable for understanding the photophysics of related hybrid amino acids or peptides clustered with Ag$_n^+$ or Au$_n^+$ clusters. In previous seminal works, it has been shown that complexation of Ag$^+$,[31] Au$^+$,[32] and Ag$_n^{+}$[33−36] with amino acids and small peptides significantly changes the optical properties of the system. In those cases, it was manifested as a strong absorption band at around the 300−450 nm spectral region attributed to charge-transfer (CT) excitation. For more information on this topic, readers are referred to a very recent and complete review that deals with these systems from basics toward sensor development.[37]

Here, we report the spectroscopic characterization in the UV region, where the nucleobase is expected to absorb, of the (cytosine)$_2$−Ag$^+$ complex (C$_2$Ag$^+$) and the related protonated cluster (C$_2$H$^+$) for comparison of their optical properties, as a reductionist approach to gain information about the molecular mechanism that controls the appealing photophysical properties of hybrid DNA−Ag$_n$ clusters. It must be noted that although it was recently established that fluorescent DNA−Ag$_n$ clusters do contain varying amounts of cationic silver, the presence of neutral silver clusters is crucial for emission of photons following excitation.[38] Thus, a direct connection between the present results and fluorescent DNA−Ag$_n$ clusters is not feasible at this point, and more work considering the hemireduced silver cluster is necessary. However, it constitutes a first approach to start understanding this interesting phenomenon.

The photofragmentation spectra of C$_2$H$^+$ and C$_2$Ag$^+$ recorded in the spectral range of 225−320 nm under similar experimental conditions for comparison are shown in Figure 1. In both cases, the main fragmentation channel was the elimination of one neutral cytosine molecule.
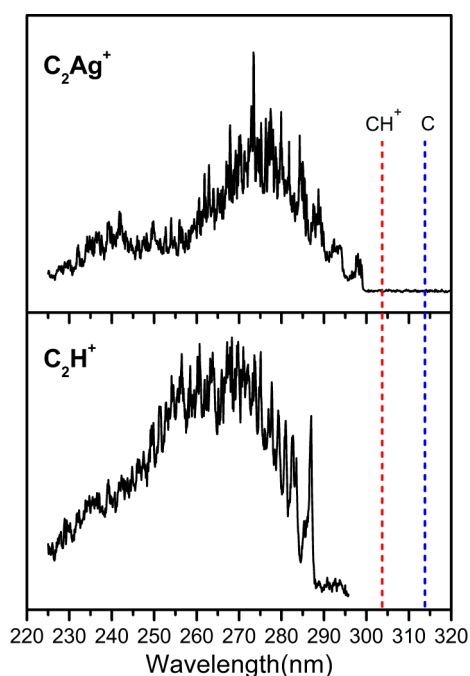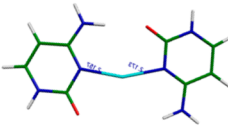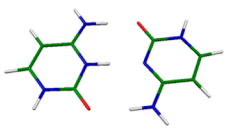

Figure 1. Photofragmentation spectra of the C$_2$Ag$^+$ and C$_2$H$^+$ complexes in the whole spectral range analyzed in this work (225−320 nm). Vertical dashed lines show the wavelengths of the origins of the electronic transition of the individual components of both complexes, C[39] and CH$^+$.[30] The electronic transition wavelengths of Ag (328.2 nm)[40] and Ag$^+$ (110.7, 111.2, and 119.6 nm)[41,42] fall out of scale.

The origins of the electronic transitions, 286.9 nm for C$_2$H$^+$ and 299.1 nm for C$_2$Ag$^+$, are close and also similar to the origin of the electronic transition of CH$^+$ (303.5 nm)[30] and C (314.2 nm).[39] An enlarged view of the spectra near the origin is shown in Figure 2, from which a very different vibronic structure and bandwidth can be observed for C$_2$H$^+$ and C$_2$Ag$^+$. The spectrum of the C$_2$Ag$^+$ complex shows a very low vibrational frequency progression at $\nu = 24$ cm^{-1} and another one at 123 cm^{-1}, which
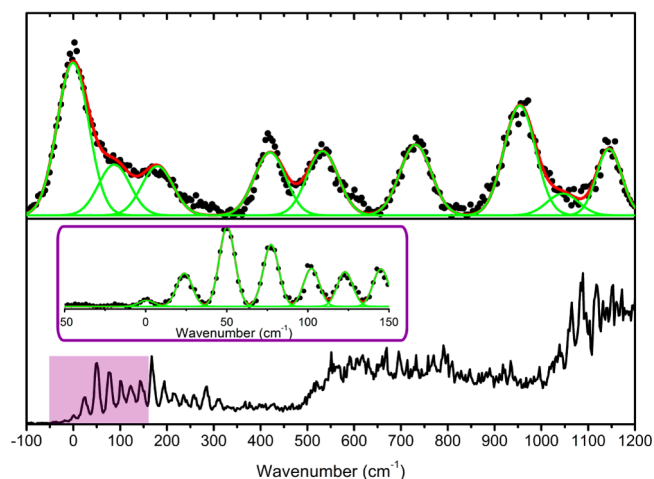
Figure 2. Low-energy part of the spectra of the C$_2$H$^+$ (upper panel) and C$_2$Ag$^+$ (lower) complexes. In the lower panel, the inset shows an amplification with better resolution of the first 150 cm^{-1} of the spectrum of the C$_2$Ag$^+$ complex, in which a low vibrational frequency progression composed of narrow bands is observed. The vibrational bands were fitted to Voigt profiles.

2296

dx.doi.org/10.1021/jz5009455 | *J. Phys. Chem. Lett.* 2014, 5, 2295−2301

Table 1. Experimental and Theoretical Electronic Excitation Energies of C_2Ag^+ and C_2H^+ Clusters for the First A′ and A″ Symmetry Excited Electronic States in Planar C_s Symmetry

	C_2Ag^+			C_2H^+		
	0-0$_{exp}$ = 4.16 eV			0-0$_{exp}$ = 4.32 eV		
	S_0[a]	$1A'(1)$[a]	$1A''(1)$[a]	S_0[a]	$1A'(1)$[a]	$1A''(1)$[a]
Osc. Strength		0.15	0.011		0.13	0.0004
S_0 optimization	0.00	4.79	4.88	0.00	4.92	5.82
A′ optimization	1.10	**4.10**	3.93	0.52	**4.44**	5.31
A″ optimization	2.00	5.32	**3.04**	3.29	6.11	**3.63**

[a]Excitation energy values are in eV.

correspond to in-plane intermolecular bending modes (N−Ag$^+$−N angle) ν_2= 33 cm^{-1} and ν_5= 95 cm^{-1}, as calculated in the ground-state geometry at the MP2/SV(P) theory level (see Figure S1 in the Supporting Information). It should be noted that this angle changes from 159° in the ground-state-optimized geometry to 165° in the A′-state-optimized geometry, which is the main geometrical change between both equilibrium structures.

The excited-state lifetimes have been estimated, as in a previous study,[30] from the widths of the bands fitted to Voigt profiles to account for the rotational contour and the laser Gaussian bandwidth (11 cm^{-1}) convolution. The intrinsic Gaussian profile of the laser is shown in Figure S2 (Supporting Information) along with the experimental profiles recorded for both complexes. The relationship between the Lorentzian full width at half-maximum (fwhm) and the excited-state lifetime (τ) is given by the uncertainty principle, which can be written as

$$\text{fwhm (cm}^{-1}) = (2\pi c \tau)^{-1} = \frac{5.3 \times 10^{-12}}{\tau \text{ (s)}} \quad (1)$$

where c stands for the speed of the light. This procedure is valid if it can be assumed that the broadening is only due to the excited-state lifetime and not to spectral congestion (e.g., rotational contour or low-frequency active vibrational modes). The spectrum of the C_2Ag^+ complex clearly shows that the spectral resolution is good enough to resolve the different vibronic transitions, even in the case of vibrational frequencies as low as 24 cm^{-1}, while the rotational broadening can be neglected because the temperature of the experiment is low (40 K).[30] Therefore, the broadening in the C_2H^+ spectrum is due to a nonradiative process leading to a short excited-state lifetime. From the bandwidth analysis, the Lorentzian fwhm for the C_2Ag^+ complex is less than 1 cm^{-1} and can be associated with an excited-state lifetime of $\tau > 5000$ fs, while the bandwidth for

the C_2H^+ complex is fwhm = 62 cm^{-1} with an associated lifetime of $\tau \approx 85$ fs, which is at least 2 orders of magnitude shorter than that of the former complex. This remarkable difference shows the effect of the Ag$^+$ cation on the excited-state dynamics of the complex. The long excited-state lifetime estimated for the C_2Ag^+ complex is compatible with the high fluorescence quantum yield of DNA−Ag$_n$ clusters with C-rich oligonucleotide strands.[9,10,14,16] The lifetime of the C_2H^+ complex is quite similar to the ones observed for the free protonated cytosine, 133 ± 20 fs,[30] indicating that it is not strongly perturbed by the dimer formation.

The electronic ground-state structures of the protonated cytosine dimer[43,44] and modified cytosine dimer[43−45] and C_2Ag^{+46} in the gas phase have been previously determined by infrared multiphoton dissociation (IR-MPD) spectroscopy together with quantum chemical calculations. Both complexes are planar (C_s symmetry) and have equivalent structures, in which each C molecule is found in the keto-amino form, with the NH groups where the glycosidic bonds are expected in transoid orientation as in the case of the *i*-motif structure of DNA. The H$^+$ as well as the Ag$^+$ cation acts as a bridge between the heteronitrogen atoms in each C (Table 1). In addition, theoretical calculations have shown that these structures are the most stable ones in the electronic ground state.[43,44,46,47]

To help the interpretation of the results and get more insight into the structure and excited-state dynamics of these complexes, ground- and excited-state optimizations were performed at the MP2 and RI-ADC(2) (SV(P) basis set) theory levels, respectively.

The ground-state optimization at the MP2 level leads to the same planar structures as that in previous studies at other levels of theory.[43,44,46,47] The vertical energies (E_{vert}) of the first excited states of A′ (symmetrical versus the molecular plane) and A″ (antisymmetrical versus the molecular plane) symmetry were also calculated (Table 1).

In many free neutral or protonated DNA bases, the S_1 optimization leads to out-of-plane deformations and to an avoided crossing between S_1 and S_0 states, which is responsible for a fast nonradiative decay.[48] For the C_2H^+ and C_2Ag^+ complexes, the size and complexity of the systems imposed a limit on the calculation to the accessible Franck–Condon region; therefore, the excited states were only optimized in C_s (planar) symmetry because the ground-state geometry is planar. Moreover, with the A″ and A′ states being very close in energy, any optimization without C_s symmetry leads to calculation failure.

The optimization of the geometry in the A′ and A″ excited states allows determination of the equilibrium (lowest-energy) structure in each excited state and then the C_s adiabatic transition energies (E_{ad}), which is the energy involved to reach the equilibrium geometry in the excited state from the equilibrium geometry in the ground state. Because the ground state is planar, they can be considered as the adiabatic potential accessible in the Franck–Condon window from the ground states, and indeed, the calculated E_{ad} values are in good agreement with the experimental transition energies ($0–0_{exp}$). All of the results are summarized in Table 1 and Figure 3. As usual for this type of calculations, the calculated adiabatic values are within 0.2 eV from the experimental ones.[30]
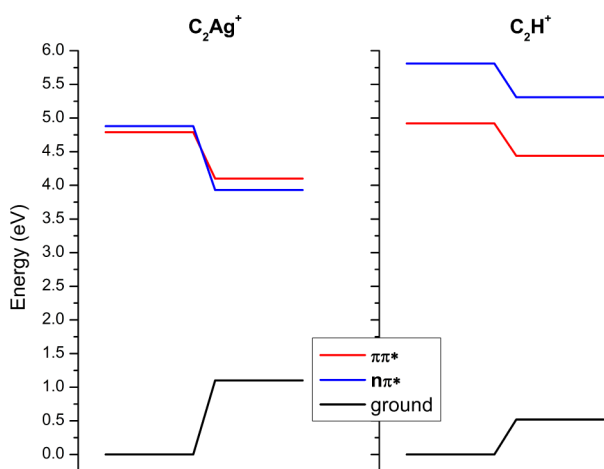
Figure 3. Scheme of the energy levels of C_2Ag^+ and C_2H^+. For each complex, the left side corresponds to the vertical energies at the ground-state equilibrium geometry, and the right side corresponds to the energies of the ground, $\pi\pi^*$, and $n\pi^*$ states at the A′($\pi\pi^*$) excited-state-optimized structure conserving the planar geometry. In the C_2Ag^+ complex, the $\pi\pi^*$ and $n\pi^*$ states are very close in energy, which might be related to the observed longer lifetime as compared with the C_2H^+ complex.

Highlighted in bold-black are the E_{ad} from the S_0 to the first A″ excited state, and in bold-red are those that best match with the experimental values of the 0−0 transition that correspond to the transition from the S_0 to the first A′ symmetry excited state in both complexes. The locally excited electronic state (A′ symmetry) is a $\pi\pi^*$ state in the C_2H^+ case, while for C_2Ag^+, in addition, it has a small partial CT character between both cytosine molecules (Figure 4).

In the case of the C_2Ag^+ complex, at the ground-state equilibrium geometry, the $\pi\pi^*$ state (A′) is lower in energy than the first (A″) $n_{Ag}\pi^*$ state. Upon excited-state optimization of the A′ states in C_s symmetry, the first A″ state becomes lower in energy than the optically allowed A′ state (Figure 3). We
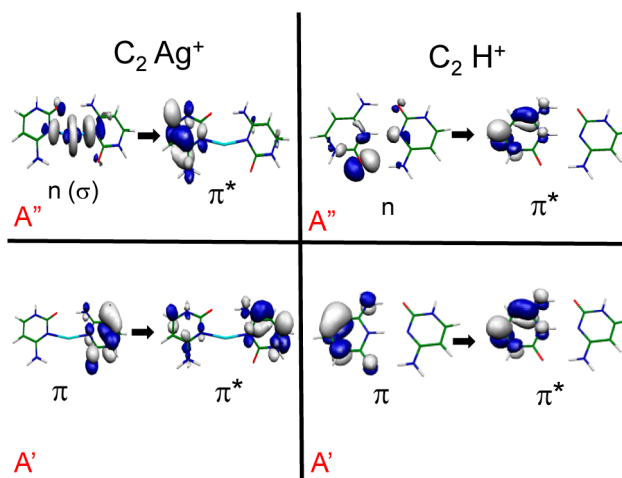
Figure 4. Main orbitals involved in the electronic structure of the two first states of A′ and A″ symmetry.

have observed a similar behavior between two tautomers of protonated uracil; the enol/enol tautomer has a short excited-state lifetime, while the enol/keto has a longer one.[30] In this latter tautomer, the $n\pi^*$ is lower in energy than the $\pi\pi^*$ at the C_s $\pi\pi^*$ optimized geometry as in the case of C_2Ag^+. Upon slight out-of-plane deformation, the optimization process of the "A″ state" brings it back in its planar geometry, while the "A′ state" tends to be stabilized upon out-of-plane deformation. This may lead to a crossing between these states and to a barrier along the out-of-plane deformation coordinate.

On the other hand, in the case of the C_2H^+ complex, the $n_O\pi^*$ state (A″) stays higher in energy than the $\pi\pi^*$ (A′) upon optimization of the A′ states in C_s symmetry. In absence of C_s symmetry, both states are mixed, and optimization of the S_1 state leads to a crossing with the ground state. Maybe there is a correlation between the energy gap between the $\pi\pi^*$ and the $n\pi^*$, the lifetime being longer when the $n\pi^*$ is slightly lower in energy at the $\pi\pi^*$ optimized geometry than when the $n\pi^*$ is higher in energy. This should be tested theoretically but on simpler systems with less spectral congestion.

One may tentatively rationalize the variation of the excited-state lifetime in the following way. The optical excitation prepares the $\pi\pi^*$ state in its C_s optimized geometry, that is, planar or nearly planar. If there is no $n\pi^*$ state lower in energy, the S_1 $\pi\pi^*$ state will easily undergo out-of-plane deformations, which leads to internal conversion. At the opposite, if the $n\pi^*$ is lower in energy than the $\pi\pi^*$ state, out-of-plane deformations will induce a crossing between these states, resulting in a barrier for the $\pi\pi^*$ state along the out-of-plane coordinate that will prevent the second crossing with the ground state at low excitation energies. Thus, this state should have a longer lifetime.

This idea has to be tested by more elaborate calculations on this system or even on the simplest protonated DNA bases for which there is now some experimental information.[30]

In summary, the complexation of two cytosine molecules with Ag^+ does not change drastically the character and energy of the electronic transition as compared to C_2H^+ or CH^+, contrary to the silver/gold amino acids case, for which a new absorption band appears in the near-UV/visible spectral region (300−450 nm), depending on the specific system, attributed to CT excitations.[31−37] The present results are in agreement with previous results[17] that suggested that in bulk systems, the UV

excitation of highly fluorescent DNA−Ag$_n$ clusters is due to absorption of the DNA bases. On the other hand, the Ag$^+$ complexation significantly changes the excited-state lifetime of the complex as compared with H$^+$ complexation. This change is explained as a consequence of the removal of a conical intersection between the excited and the ground states of the C$_2$Ag$^+$ complex, which takes place in the C$_2$H$^+$ complex and leads to a fast nonradiative decay of the excited state of the latter. Therefore, a higher fluorescence quantum yield is expected upon Ag$^+$ complexation, and this could be the reason for the high fluorescence of DNA−Ag$_n$ clusters, although in the latter case, the fluorescence is observed upon chemical reduction of Ag$^+$. However, it has been shown that cationic systems can give relevant and detailed information to understand the optical properties of hybrid biomolecule− noble metal clusters.[31−37]

The ultimate goal of noble metal bioconjugation is to develop biosensing at the molecular level, and gas-phase studies can help to build model systems in a bottom-up strategy. In this regard, the next step will be to generate larger Ag$_n^+$ clusters conjugated with DNA bases, in which some reduction processes have taken place.

■ METHODOLOGY

(a) *Experiment.* The electronic spectra of the C$_2$Ag$^+$ and C$_2$H$^+$ complexes were obtained via parent ion photofragment spectroscopy in a cryogenically cooled quadrupole ion trap (Paul trap from Jordan TOF Products, Inc.).[49] The setup is similar to the one developed in several groups based on the original design by Wang and Wang.[50−52] The complexes are produced in an electrospray ionization source built at Aarhus University[53] by introducing a solution of cytosine (500 μM) and silver nitrate (250 μM) in a methanol (50%)/water (50%) solvent. At the exit of the capillary, ions are trapped in an octopole trap for 90 ms. They are extracted by applying a negative pulse of ∼50 V and are further accelerated to 190 V by a second pulsed voltage just after the exit electrode. This time sequence of pulsed voltages produces ion packets with duration between 500 ns and 1 μs. The ions are driven by a couple of electrostatic lenses toward the Paul trap biased at 190 V so that the ions enter the trap gently avoiding fragmentation induced by collisions. A mass gate placed at the entrance of the trap allows selection of the parent ion. The Paul trap is mounted on the cold head of a cryostat (Coolpak Oerlikon) connected to a water-cooled He compressor. Helium as buffer gas is injected in the trap using a pulsed valve (General Valve) triggered 1 ms before the ions enter the trap, as previously reported by Kamrath et al.[51] The ions are trapped and thermalized at a temperature between 20 and 50 K through collisions with the cold buffer gas. The ions are kept in the trap for several tens of milliseconds before the photodissociation laser is triggered. This delay is necessary to ensure thermalization of ions and efficient pumping of the He buffer gas from the trap to avoid collision-induced dissociation of the ions during the extraction toward the 1.5 m long time-of-flight (TOF) mass spectrometer. After laser excitation, the ions are stored in the trap for a delay that can be varied between 20 and 90 ms before extraction to the TOF mass spectrometer. The complete mass spectrum is recorded on a microchannel plate (MCP) detector with a digitizing storage oscilloscope interfaced to a PC. The photofragment yield spectrum of each detected ion is normalized to the parent ion signal and the laser power. The photodissociation laser is an OPO laser from EKSPLA, which

has a 10 Hz repetition rate, 10 ns pulse width, resolution of 10 cm^{-1}, and scanning step of 0.02 nm. The laser is shaped to a 1 mm^2 spot to fit the entrance hole of the trap, and the laser power is around 20 mW in the UV spectral region.

(b) *Calculations.* Ab initio calculations have been performed with the TURBOMOLE program package,[54] making use of the resolution-of-the-identity (RI) approximation for the evaluation of the electron-repulsion integrals.[55] The equilibrium geometry of the clusters and the vibrational frequencies in their ground electronic state (S$_0$) were determined at the MP2/SV(P) level. The excitation energy and equilibrium geometry of the lowest excited singlet state (S$_1$) were determined at the RI-ADC(2)/ SV(P) level.

Structure optimizations were done by the quasi-Newton− Raphson methods using the exact gradient vector and an approximation to the Hessian matrix as implemented in the TURBOMOLE program package.

■ ASSOCIATED CONTENT

ⓈSupporting Information

Description and assignment of the low-frequency vibrational active modes of the C$_2$Ag$^+$ cluster and the intrinsic Gaussian profile of the laser together with the experimental profiles recorded for both complexes. This material is available free of charge via the Internet at http://pubs.acs.org.

■ AUTHOR INFORMATION

Corresponding Author
*E-mail: gpino@fcq.unc.edu.ar.

Notes

The authors declare no competing financial interest.

■ ACKNOWLEDGMENTS

■ REFERENCES

(1) Seeman, N. C. DNA in a Material World. *Nature* 2003, *421*, 427−431.

(2) Li, X.; Liu, D. R. DNA-Templated Organic Synthesis: Nature's Strategy for Controlling Chemical Reactivity Applied to Synthetic Molecules. *Angew. Chem., Int. Ed.* 2004, *43*, 4848−4870.

(3) Lu, Y.; Liu, J. Functional DNA Nanotechnology: Emerging Applications of DNAzymes and Aptamers. *Curr. Opin. Biotechnol.* 2006, *17*, 580−588.

(4) Feldkamp, U.; Niemeyer, C. M. Rational Design of DNA Nanoarchitectures. *Angew. Chem., Int. Ed.* 2006, *45*, 1856−1876.

(5) Niemeyer, C. M.; Mirkin, C. A. *Nanobiotechnology: Concepts, Applications and Perspectives*; Wiley-VCH: Weinheim, Germany, 2004.

(6) Takezawa, Y.; Shionoya, M. Metal-Mediated DNA Base Pairing: Alternatives to Hydrogen-Bonded Watson−Crick Base Pairs. *Acc. Chem. Res.* 2012, *45*, 2066−2076.

(7) Liu, S.; Clever, G. H.; Takezawa, Y.; Kaneko, M.; Tanaka, K.; Guo, X.; Shionoya, M. Direct Conductance Measurement of Individual Metallo-DNA Duplexes within Single-Molecule Break Junctions. *Angew. Chem., Int. Ed.* 2011, *50*, 8886−88890.

(8) Park, K. S.; Jung, C.; Park, H. G. "Illusionary" Polymerase Activity Triggered by Metal Ions: Use for Molecular Logic-Gate Operations. *Angew. Chem., Int. Ed.* 2010, *49*, 9757−9760.

(9) Miyake, Y.; Togashi, H.; Tashiro, M.; Yamaguchi, H.; Oda, S.; Kudo, M.; Tanaka, Y.; Kondo, Y.; Sawa, R.; Fujimoto, T.; et al.

2299

dx.doi.org/10.1021/jz5009455 | *J. Phys. Chem. Lett.* 2014, 5, 2295−2301

Mercury II-Mediated Formation of Thymine−HgII−Thymine Base Pairs in DNA Duplexes. *J. Am. Chem. Soc.* **2006**, *128*, 2172−2173.

(10) Ono, A.; Shiqi, C.; Humika, T.; Tashiro, M.; Fujimoto, T.; Machinami, T.; Oda, S.; Miyake, Y.; Okamoto, I.; Tanaka, Y. Specific Interactions between Silver(I) Ions and Cytosine−Cytosine Pairs. *Chem. Commun.* **2008**, *44*, 4825−4827.

(11) Urata, H.; Yamaguchi, E.; Nakamura, Y.; Wada, S. Pyrimidine−Pyrimidine Base Pairs Stabilized by Silver(I) Ions. *Chem. Commun.* **2011**, *47*, 941−943.

(12) Zheng, Y.; Yang, C.; Yang, F.; Yang, X. Real-Time Study of Interactions between Cytosine−Cytosine Pairs in DNA Oligonucleotides and Silver Ions Using Dual Polarization Interferometry. *Anal. Chem.* **2014**, *86*, 3849−3855.

(13) Xu, G.; Wang, G.; He, X.; Zhu, Y.; Chen, L.; Zhang, X. An Ultrasensitive Electrochemical Method for Detection of Ag^+ Based on Cyclic Amplification of Exonuclease III Activity on Cytosine−Ag^+−Cytosine. *Analyst* **2013**, *138*, 6900−6906.

(14) Petty, J. T.; Story, S. P.; Hsiang, J. C.; Dickson, R. M. DNA-Templated Molecular Silver Fluorophores. *J. Phys. Chem. Lett.* **2013**, *4*, 1148−1155.

(15) Richards, C. I.; Choi, S.; Hsiang, J.; Antoku, Y.; Vosch, T.; Bongiorno, A.; Tzeng, Y.; Dickson, R. M. Oligonucleotide-Stabilized Ag Nanocluster Fluorophores. *J. Am. Chem. Soc.* **2008**, *8*, 5038−5039.

(16) Petty, J. T.; Sergev, O. O.; Nicholson, D. A.; Goodwin, P. M.; Giri, B.; McMullan, D. R. A Silver Cluster−DNA Equilibrium. *Anal. Chem.* **2013**, *85*, 9868−9876.

(17) O'Neill, P. R.; Gwinn, E. G.; Fygenson, D. K. UV Excitation of DNA Stabilized Ag Cluster Fluorescence via the DNA Bases. *J. Phys. Chem. C* **2011**, *115*, 24061−24066.

(18) Copp, S. M.; Schultz, D.; Swasey, S.; Pavlovich, J.; Debord, M.; Chiu, A.; Olsson, K.; Gwinn, E. Magic Numbers in DNA-Stabilized Fluorescent Silver Clusters Lead to Magic Colors. *J. Phys. Chem. Lett.* **2014**, *5*, 959−963.

(19) Ritchie, C. M.; Johnsen, K. R.; Kiser, J. R.; Antoku, Y.; Dickson, R. M.; Petty, J. T. Ag Nanocluster Formation Using a Cytosine Oligonucleotide Template. *J. Phys. Chem. C* **2007**, *111*, 175−181.

(20) Oemrawsingh, S. S. R.; Markešević, N.; Gwinn, E. G.; Eliel, E. R.; Bouwmeester, D. Spectral Properties of Individual DNA-Hosted Silver Nanoclusters at Low Temperatures. *J. Phys. Chem. C* **2012**, *116*, 25568−25575.

(21) Vosch, T.; Antoku, Y.; Hsiang, J.; Richards, C. I.; Gonzalez, J. I.; Dickson, R. M. Strongly Emissive Individual DNA-Encapsulated Ag Nanoclusters as Single-Molecule Fluorophores. *Proc. Natl. Acad. Sci. U.S.A.* **2007**, *104*, 12616−12621.

(22) Choi, S.; Dickson, R. M.; Yu, J. Developing Luminescent Silver Nanodots for Biological Applications. *Chem. Soc. Rev.* **2012**, *41*, 1867−1891.

(23) Díez, I.; Ras, R. H. a. Fluorescent Silver Nanoclusters. *Nanoscale* **2011**, *3*, 1963−1970.

(24) Xu, H.; Suslick, K. S. Water-Soluble Fluorescent Silver Nanoclusters. *Adv. Mater.* **2010**, *22*, 1078−1082.

(25) Guo, S.; Wang, E. Noble Metal Nanomaterials: Controllable Synthesis and Application in Fuel Cells and Analytical Sensors. *Nano Today* **2011**, *6*, 240−264.

(26) Shang, L.; Dong, S.; Nienhaus, G. U. Ultra-Small Fluorescent Metal Nanoclusters: Synthesis and Biological Applications. *Nano Today* **2011**, *6*, 401−418.

(27) Latorre, A.; Somoza, Á. DNA-Mediated Silver Nanoclusters: Synthesis, Properties and Applications. *ChemBioChem* **2012**, *13*, 951−958.

(28) Petty, J. T.; Zheng, J.; Hud, N. V.; Dickson, R. M. DNA-Templated Ag Nanocluster Formation. *J. Am. Chem. Soc.* **2004**, *126*, 169−173.

(29) Kleinermanns, K.; Nachtigallová, D.; de Vries, M. S. Excited State Dynamics of DNA Bases. *Int. Rev. Phys. Chem.* **2013**, *32*, 308−342.

(30) Berdakin, M.; Dedonder-Lardeux, C.; Jouvet, C.; Pino, G. A. Excited States of Protonated DNA/RNA Bases. *Phys. Chem. Chem. Phys.* **2014**, *16*, 10643−10650.

(31) Antoine, R.; Tabarin, T.; Broyer, M.; Dugourd, P.; Mitric, R.; Bonačić-Koutecký, V. Optical Properties of Gas-Phase Tryptophan−Silver Cations: Charge Transfer from the Indole Ring to the Silver Atom. *ChemPhysChem* **2006**, *7*, 524−528.

(32) Antoine, R.; Bertorelle, F.; Broyer, M.; Compagnon, I.; Dugourd, P.; Kulesza, A.; Mitric, R.; Bonačić-Koutecký, V. Gas-Phase Synthesis and Intense Visible Absorption of Tryptophan−Gold Cations. *Angew. Chem., Int. Ed.* **2009**, *48*, 7829−7832.

(33) Compagnon, I.; Tabarin, T.; Antoine, R.; Broyer, M.; Dugourd, P. Spectroscopy of Isolated, Mass-Selected Tryptophan−Ag_3 Complex: A Model for Photoabsorption Enhancement in Nanoparticle−Biomolecule Hybrid Systems. *J. Chem. Phys.* **2006**, *125*, 164326−164331.

(34) Mitrić, R.; Petersen, J.; Kulesza, A.; Bonačić-Koutecký, V.; Tabarin, T.; Compagnon, I.; Antoine, R.; Broyer, M.; Dugourd, P. Photoabsorption and Photofragmentation of Isolated Cationic Silver Cluster−Tryptophan Hybrid Systems. *J. Chem. Phys.* **2007**, *127*, 134301/1−13401/10.

(35) Mitrić, R.; Petersen, J.; Kulesza, A.; Bonačić-Koutecký, V.; Tabarin, T.; Compagnon, I.; Antoine, R.; Broyer, M.; Dugourd, P. Absorption Properties of Cationic Silver Cluster−Tryptophan Complexes: A Model for Photoabsorption and Photoemission Enhancement in Nanoparticle−Biomolecule Systems. *Chem. Phys.* **2008**, *343*, 372−380.

(36) Sanader, Z.; Mitrić, R.; Bonačić-Koutecký, V.; Bellina, B.; Antoine, R.; Dugourd, P. The Nature of Electronic Excitations at the Metal−Bioorganic Interface Illustrated on Histidine−Silver Hybrids. *Phys. Chem. Chem. Phys.* **2014**, *16*, 1257−1261.

(37) Bonačić-Koutecký, V.; Kulesza, A.; Gell, L.; Mitrić, R.; Antoine, R.; Bertorelle, F.; Hamouda, R.; Rayane, D.; Broyer, M.; Tabarin, T.; et al. Silver Cluster−Biomolecule Hybrids: From Basics towards Sensors. *Phys. Chem. Chem. Phys.* **2012**, *14*, 9282−9290.

(38) Schultz, D.; Gardner, K.; Oemrawsingh, S. S. R.; Markešević, N.; Olsson, K.; Debord, M.; Bouwmeester, D.; Gwinn, E. Evidence for Rod-Shaped DNA-Stabilized Silver Nanocluster Emitters. *Adv. Mater.* **2013**, *25*, 2797−2803.

(39) De Vries, M. S.; Hobza, P. Gas-Phase Spectroscopy of Biomolecular Building Blocks. *Annu. Rev. Phys. Chem.* **2007**, *58*, 585−612.

(40) Fuhr, J. R.; Wiese, W. L. *CRC Handbook of Chemistry and Physics*; CRC Press: Boca Raton, FL, 1998.

(41) Biémont, E.; Pinnington, E. H.; Kernahan, J. A.; Rieger, G. Beam-Laser Measurements and Relativistic Hartree−Fock Calculations of the Lifetimes of the $4d^9 5p$ Levels in Ag II. *J. Phys. B* **1997**, *30*, 2067−2073.

(42) Kramida, A. A Critical Compilation of Energy Levels, Spectral Lines, and Transition Probabilities of Singly Ionized Silver, Ag II. *J. Res. Natl. Inst. Stand. Technol.* **2013**, *118*, 168−198.

(43) Yang, B.; Rodgers, M. T. Base-Pairing Energies of Proton-Bound Heterodimers of Cytosine and Modified Cytosines: Implications for the Stability of DNA I-Motif Conformations. *J. Am. Chem. Soc.* **2013**, *136*, 282−290.

(44) Yang, B.; Wu, R. R.; Berden, G.; Oomens, J.; Rodgers, M. T. Infrared Multiple Photon Dissociation Action Spectroscopy of Proton-Bound Dimers of Cytosine and Modified Cytosines: Effects of Modifications on Gas-Phase Conformations. *J. Phys. Chem. B* **2013**, *117*, 14191−14201.

(45) Oomens, J.; Moehlig, A. R.; Morton, T. H. Infrared Multiple Photon Dissociation (IRMPD) Spectroscopy of the Proton-Bound Dimer of 1-Methylcytosine in the Gas Phase. *J. Phys. Chem. Lett.* **2010**, *1*, 2891−2897.

(46) Berdakin, M.; Steinmetz, V.; Maitre, P.; Pino, G. A. Gas Phase Structure of Metal Mediated (Cytosine)$_2$Ag$^+$ Mimics the Hemi-protonated (Cytosine)$_2$H$^+$ Dimer in I-Motif Folding. *J. Phys. Chem. A* **2014**, *118*, 3804−3809.

(47) Megger, D. A.; Fonseca Guerra, C.; Bickelhaupt, F. M.; Müller, J. Silver(I)-Mediated Hoogsteen-Type Base Pairs. *J. Inorg. Biochem.* **2011**, *105*, 1398−1404.

(48) Delchev, B. V.; Sobolewskib, A. L.; Domckea, W. Comparison of the Non-Radiative Decay Mechanisms of 4-Pyrimidinone and Uracil: An Ab Initio Study. *Phys. Chem. Chem. Phys.* **2010**, *12*, 5007−5015.

(49) Alata, I.; Bert, J.; Broquier, M.; Dedonder, D.; Feraud, G.; Grégoire, G.; Soorkia, S.; Marceca, E.; Jouvet, C. J. Electronic Spectra of the Protonated Indole Chromophore in the Gas Phase. *J. Phys. Chem. A* **2013**, *117*, 4420−4427.

(50) Wang, X. B.; Wang, L. S. Development of a Low-Temperature Photoelectron Spectroscopy Instrument Using an Electrospray Ion Source and a Cryogenically Controlled Ion Trap. *Rev. Sci. Instrum.* **2008**, *79*, 073108−073109.

(51) Kamrath, M. Z.; Relph, R. A.; Guasco, T. L.; Leavitt, C. M.; Johnson, M. A. Vibrational Predissociation Spectroscopy of the H_2-Tagged Mono- and Dicarboxylate Anions of Dodecanedioic Acid. *Int. J. Mass Spectrom.* **2011**, *300*, 91−98.

(52) Choi, C. M.; Kim, H. J.; Lee, J. H.; Shin, W. J.; Yoon, T. O.; Kim, N. J.; Heo, J. Ultraviolet Photodepletion Spectroscopy of Dibenzo-18-Crown-6-Ether Complexes with Alkali Metal Cations. *J. Phys. Chem. A* **2009**, *113*, 8343−8350.

(53) Andersen, J. U.; Cederquist, H.; Forster, J. S.; Huber, B. A.; Hvelplund, P.; Jensen, J.; Liu, B.; Manil, B.; Maunoury, L.; Brøndsted Nielsen, S.; et al. Photodissociation of Protonated Amino Acids and Peptides in an Ion Storage Ring. Determination of Arrhenius Parameters in the High-Temperature Limit. *Phys. Chem. Chem. Phys.* **2004**, *6*, 2676−2681.

(54) Ahlrichs, R.; Bär, M.; Häser, M.; Horn, H.; Kölmel, C. Electronic Structure Calculations on Workstation Computers: The Program System Turbomole. *Chem. Phys. Lett.* **1989**, *162*, 165−169.

(55) Hättig, C. Geometry Optimizations with the Coupled-Cluster Model CC2 Using the Resolution-of-the-Identity Approximation. *J. Chem. Phys.* **2003**, *118*, 7751−7761.